THERMAL BEHAVIOR OF ENZYMATIC HYDROLYSIS LIGNIN BASED ON TG-FTIR ANALYSIS

XIAOJUN ZHU,[#] YUGUO DONG,[#] XINYU LU, HAN QUE,
YIMENG ZHANG[*] and XIAOLI GU

College of Chemical Engineering, Nanjing Forestry University, Nanjing 210037, China
[*]*College of Materials Science and Engineering, Nanjing Forestry University, Nanjing 210037, China*
[#]*Both authors contributed equally to this work*
✉ *Corresponding authors: Xiaoli Gu, guxiaoli@njfu.edu.cn*
Yimeng Zhang, njfugxl@126.com

Received April 16, 2018

The thermal decomposition of enzymatic hydrolysis lignin (EHL) was investigated by the thermogravimetric technique (TG/DTG) within the temperature range from room temperature to 920 °C at different heating rates (10, 20, 30, 40 and 50 °C/min). Little differences in the mass losses as a function of the heating rates were observed from TG analysis. It was established that EHL pyrolysis consisted of three main stages: water evaporation (<200 °C), devolatilization of organic volatiles (200-500 °C) and char formation (>500 °C). The evolved gases or volatiles were investigated by Fourier transform infrared spectrometry (FTIR), coupled to a thermo-balance, at the heating rate of 20 °C/min, for identifying the gaseous or volatile species and their evolution during EHL thermal degradation. The temperatures corresponding to the maximum evolution rate of H_2O, CO_2, CO, CH_4 and C_2H_4, as well as the volatile fragments originating from the breaking of covalent chemical bonds, such as C-C, C=O and C-O-C groups, were in agreement with the temperature corresponding to the maximum mass loss rate – of about 385~400 °C. The maximum release rates of H_2O, CO_2, CO, CH_4 and C_2H_4 took place at 387, 385, 392, 392 and 389 °C, respectively. While the maximum rates of evolution of both alkyl groups and oxygen-containing compounds occurred at about 400 °C. The kinetic processing of non-isothermal TG/DTG data was performed by the model-free methods proposed by Flynn, Wall, Ozawa (known as FWO method) and Kissing, Akahira and Sunose (KAS method). The average activation energies calculated by the FWO and KAS methods were 191.2 kJ mol^{-1} and 191.0 kJ mol^{-1}, respectively. Experimental results showed that the values of kinetic parameters obtained by both methods were analogous and thus these methods could be successfully applied to understand the complex degradation mechanism of EHL. Also, such an approach is helpful in achieving a better understanding of the devolatilization process of different types of biomass.

Keywords: enzymatic hydrolysis lignin, pyrolysis, kinetics, TG-FTIR

INTRODUCTION

A comprehensive understanding of the thermal decomposition of biomass (cellulose, hemicellulose and lignin) is of great importance in evaluating the influence of evolved gases, volatile liquids and residual solids, under pyrolysis conditions, on the thermal behavior of biomass components. Upon heating in inert atmosphere, the three-dimensional structure of lignin would undergo various changes due to the release of gases and volatiles.[1-3] Thermal analysis techniques, such as thermogravimetric analysis (TG/DTG), are often employed for studying the pyrolysis mass loss information and acquiring knowledge about kinetic parameters during thermal decomposition reactions, which are essential in investigating the lignin conversion system.[4-7] Moreover, the TG/DTG analysis techniques coupled with the analysis of evolved gases (EGA) during the thermal degradation process of lignin have very important advantages.[8] The mass changes could be correlated with the identification of volatiles or gases released during

pyrolysis.[9-11] Among various instrumentations to be coupled, Fourier transform infrared (FTIR) spectrometry is convenient and sensitive for the detection of gases or organic volatile compounds.

On the other hand, knowledge of kinetic parameters is necessary in mathematical modeling of reactor and process optimization. Currently, most methods for analyzing non-isothermal solid substrate pyrolytic kinetics from TG/DTG analysis could be divided into model-fitting and model-free (iso-conversional) methods.[12-14] Model-fitting methods (including the Freeman-Carroll method, the Coats-Redfern method *etc*.) consist in fitting different models to the data for the purpose of optimizing the best statistical model from which the kinetic parameters could be calculated. Model-free methods (including the Kissinger-Akahira-Sonuse method, the Flynn-Wall-Ozawa method *etc*.) require different kinetic curves at different heating rates to calculate the kinetic parameters on the same value of conversion. Obviously, model-free isoconversional methods are advantageous in estimating the apparent activation energy without a prior prediction of the reaction model due to their accuracy.[15,16]

Although, in the past, plenty of papers were dedicated to investigating devolatilization of lignin during thermal decomposition in inert atmosphere,[17-20] scarce detailed pyrolysis kinetics information about enzymatic hydrolysis lignin (EHL) pyrolysis could be found in the available literature. The lack of data leads to difficulties in understanding the thermal behavior of EHL.

The purpose of this paper has been to gain a deeper insight into the pyrolysis behavior of EHL for improving the thermal decomposition efficiency. The pyrolysis process was studied by TG/DTG under helium atmosphere in the temperature range from room temperature to 920 °C under non-isothermal conditions (10, 20, 30, 40 and 50 °C/min heating rates). EGA was carried out by Fourier transform infrared (FTIR) spectrometry coupled with a thermo-balance, at 20 °C/min heating rate, for identifying the gaseous or volatile species and their evolution during EHL thermal degradation. The kinetic parameters of the EHL pyrolysis process were also determined by the isoconversional method. To our knowledge, this is the most detailed thermal and kinetic characterization of EHL pyrolysis to date.

EXPERIMENTAL

Materials

The EHL sample was generated from residues of bio-ethanol production, supplied by Biological Engineering Laboratory, Nanjing Forestry University.[21] The purification of EHL was done by the alkali-solution (sodium hydroxide aqueous solution) and acid-isolation (dilute sulfuric acid solution) methods.[22] After filtration and repeated washing with distilled water, the EHL sample was dried in an oven at 105 °C for 3 h. Then, the original materials were crushed and pulverized to a size of <0.2 mm before they were analyzed.[23]

TG-FTIR quantitative analysis

TG-FTIR analysis was conducted with a PerkinElmer TGA 8000 thermogravimetric analyzer (PerkinElmer, USA) and the operational conditions were similar to those described in our former report.[24] The pyrolysis process of EHL was studied by a thermogravimetric simultaneous thermal analyzer under helium atmosphere (flow rate of 50 mL/min), temperature ranging from room temperature to 920 °C, heating rate set as 10, 20, 30, 40 and 50 °C/min. The thermal analyzer's microbalance sensitivity is less than ±0.1 μg and temperature precision is ±0.5 °C. The initial mass of the samples loaded into the crucible was 10 ± 0.5 mg to avoid heat transfer limitations. Duplicate experiments were conducted to eliminate test errors and to guarantee repeatability. Fourier transform infrared measurements were conducted by a PerkinElmer Frontier™ FTIR spectrometer coupled to a thermal analyzer (<0.1 min detention) for the identification of the gaseous species or volatiles and their evolution profiles during the pyrolysis of the substrates. The gases or volatiles evolved from TGA passed through a heated transfer line, which was heated to 285 °C in order to prevent the condensation of volatiles. The scanning range for FTIR was set to 550-4000 cm^{-1}.

Kinetics theory

The kinetics of the reaction in solid state is described by the following equation:

$$\frac{d\alpha}{dt} = k(T) f(\alpha) \quad (1)$$

Conversion, α, is the normalized form of the mass loss data of the decomposed sample and is defined as follows:

$$\alpha = 1 - \frac{m_{(t)} - m_f}{m_0 - m_f} \quad (2)$$

where $m_{(t)}$ is the experimental mass at each monitoring time, m_f is the final mass and m_0 is the initial dry mass.

According to the Arrhenius equation, the temperature dependence of the rate constant k is given

by:

$$k = A \cdot \exp(-\frac{E}{RT}) \quad (3)$$

where Ea is the activation energy (kJ mol^{-1}), T is the absolute temperature (K), R is the gas constant (8.314 J K^{-1} mol^{-1}) and A is the pre-exponential factor (min^{-1}). The combination of the two equations, *i.e.* (1) and (3), gives the fundamental expression (4) of analytical methods to calculate kinetic parameters, on the basis of TGA results:

$$\frac{d\alpha}{dt} = A \cdot f(\alpha) \cdot \exp(-\frac{E}{RT}) \quad (4)$$

The expression of the function f(α) and its derivative f'(α) = -1 are used for describing a solid-state first-order reaction, and the mathematical function f(α) could be restricted to the following expression:

$$f(\alpha) = (1-\alpha)^n \quad (5)$$

where n is the reaction order. According to the classical theory for the kinetics of chain reactions,[25] biomass thermal decomposition usually has an order of reaction of 1.0. Substituting expression (5) in Equation (4) gives the expression of the reaction rate in the form:

$$\frac{d\alpha}{dt} = A \exp(-\frac{E}{RT}) (1-\alpha)^n \quad (6)$$

For non-isothermal TGA experiments, at linear heating rate β = dT/dt, Equation (6) can be written as:

$$\frac{d\alpha}{dT} = (\frac{A}{\beta})\exp(-\frac{E}{RT})(1-\alpha)^n \quad (7)$$

This equation expresses the fraction of material consumed.

In this work, the activation energy was obtained from non-isothermal TGA. The methods used to calculate kinetic parameters are called model-free non-isothermal methods and require a set of experimental results at different heating rates.

Model-free methods

Flynn-Wall-Ozawa method

The FWO method[26,27] is an integral technique, expressed in straight lines at different heating rates according to the relationship between the logarithm of the heating rate and reciprocal temperature at constant mass loss, in which the apparent activation energy of degradation was calculated from the slope of linear relationships. This method allowed obtaining apparent activation energy (Ea_α) from a plot of the natural logarithm of heating rates, lnβ *versus* 1000/$T_{\alpha i}$, which represents the linear relation with a given value of conversion (α) at different heating rates (β). $T_{\alpha i}$ is the corresponding temperature of the DTG curve at a given conversion (shown in Fig. 1).

$$\ln(\beta_i) = \ln\frac{A_\alpha E_\alpha}{Rg(\alpha)} - 5.331 - 1.052\frac{E_\alpha}{RT_{\alpha i}} \quad (8)$$

where g(α) is constant at a given value of conversion, *e.g.*, g(α) = -ln(1-α) when n = 1.0. The subscripts i and α denote a given value of heating rate and a given value of conversion, respectively. The activation energy E_α is calculated from the slope -1.052 E_α/R.

Kissing-Akahira-Sunose method

Similarly, the KAS method[28] could also yield the value of activation energy from a plot of ln(β/$T_{\alpha i}^2$) against 1000/$T_{\alpha i}$ for a series of experiments at different heating rates (β), where $T_{\alpha i}$ is the corresponding temperature of the DTG curve at a given conversion (α). The subscripts i and α denote a given value of heating rate and a given value of conversion, respectively. The equation is based on the following expression:

$$\ln(\frac{\beta}{T_{\alpha i}^2}) = -\frac{E_\alpha}{RT_{\alpha i}} + \ln(\frac{A_\alpha R}{E_\alpha g(\alpha)}) \quad (9)$$

The apparent activation energy can be obtained from the plot of ln($\beta_i/T_{\alpha i}^2$) *versus* 1000/$T_{\alpha i}$ for a given value of conversion, α, where the slope is equal to -E_α/R.

RESULTS AND DISCUSSION

TG/DTG analysis

The TG/DTG curves obtained by heating EHL at different heating rates (10, 20, 30, 40 and 50 °C/min) in the temperature range from room temperature to 920 °C under helium atmosphere are shown in Figure 1. As shown in Figure 1a, the five mass loss curves were similar exhibiting the same decreasing tendency with the increase in temperature. The content of residual products (char) at increasing heating rates was 31.1 wt%, 32.5 wt%, 32.6 wt%, 33.3 wt% and 33.4 wt%, respectively. This trend is in accordance with the fact that the occurrence of secondary reactions, such as thermal cracking of formed transitional organic polymers, is unavoidable at increasing heating rates because of shorter reaction time. In general, the heating rate could be an important factor to affect the pyrolysis process, including mass loss, gaseous or volatile products released and so on.[29,30] Therefore, different heating rates were employed to investigate the effect of heating rate on pyrolysis.

All the thermo-analytical curves presented the same profiles, which were slightly shifting toward higher temperatures at increasing heating rates. Three principal regions of mass losses were recognized on the TG curves (Fig. 1a), *e.g.*, water

evaporation (stage I), devolatilization of organic volatiles (stage II) and char formation (stage III), whereas one main peak was identified on the corresponding derivative TG curves (see Fig. 1b). In detail, the initial decrease in mass is mainly due to water release at a temperature below 200 °C, which is related to the evaporation of moisture and adsorbed water from the substrate[31] (see stage I). The second stage is the primary pyrolysis of EHL with the formation of volatile products originating from scission of bonds in the lignin structure, as the temperature increases from 200 to 600 °C. For example, the mass decreases sharply with the maximum mass loss rate of -9.6 wt%/min at the heating rate of 20 °C/min. The temperature corresponding to the maximum mass loss rate of the sample is about 366 °C. A large amount of gas species, such as CO_2, CO, CH_4 and H_2O, are released in this stage, which indicates that they mainly come from this primary pyrolysis stage (see stage II). As the temperature continues increasing (above 600 °C), the mass variation is very small, while a lower amount of gaseous or volatile species is released and char is formed (see stage III).

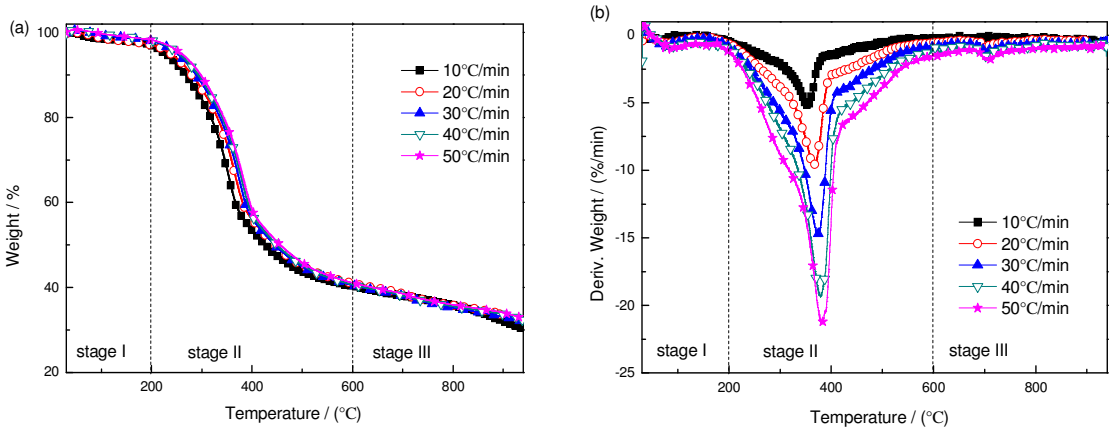

Figure 1: TG (a) and DTG (b) curves for EHL at different heating rates

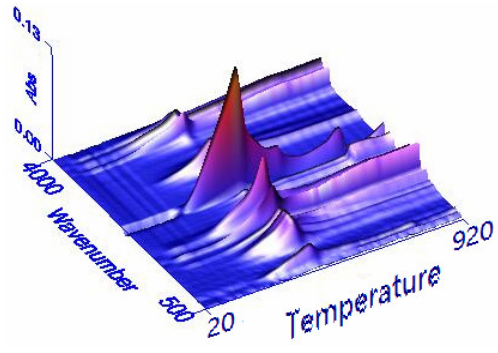

Figure 2: 3D surface graph for FTIR spectra of evolved gases and volatiles produced by devolatilization of EHL at 20 °C/min heating rate

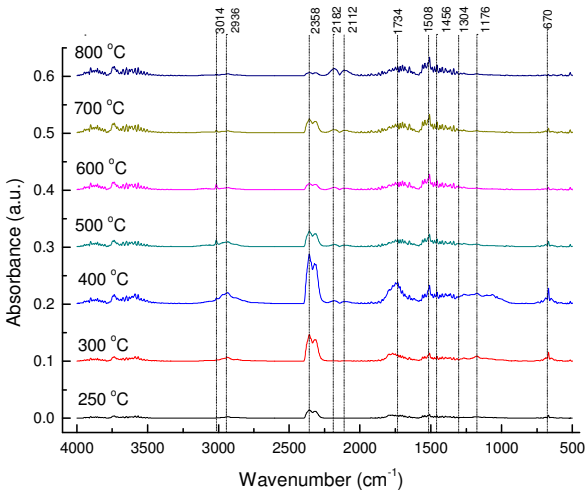

Figure 3: FTIR spectra of EHL gaseous and volatile products at different temperatures at 20 °C/min heating rate

EGA by FTIR

The results obtained from the TG/DTG analysis indicated that the proportion of the volatile content in EHL played an important role during the EHL pyrolysis process. FTIR coupled to the thermal analyzer was used for performing real-time analysis to identify the gaseous or volatile species evolved. The 3D-FTIR obtained during the devolatilization of EHL under helium atmosphere at 20 °C/min by TG-FTIR is shown in Figure 2. The FTIR spectra recorded at the temperature ranging from 250 to 800 °C are also reported in Figure 3. Based on the FTIR results, the peak of evolution taking place at the temperature of about 250 °C was mainly associated to the removal of absorbed water, originating from scissions of bonds in the lignin structure (δ(O-H) bending mode at 1508 cm^{-1}), which was accompanied with a minor amount of CO_2 (characteristic bands at 2358/670 cm^{-1}).

The most intensive peak occurring at about 400 °C was due to the evolution of CO_2, CO (characteristic double peaks at 2182/2112 cm^{-1}), and light aliphatic gases, such as methane (characteristic double bands at 3014/1304 cm^{-1}) and ethylene (characteristic double bands at 1456 cm^{-1}). Moreover, most overlapped vibrational bands of alkyl groups attached to the aromatic hydrocarbons and aliphatic chains were evidenced in the IR region of 3100-2800 cm^{-1}. The C-O stretching vibration between 1100 and 1300 cm^{-1}, attributed to phenols, alcohols and ethers, was also seen. The FTIR spectra corresponding to the evolution peaks at 300, 400, 500, 600 and 700 °C showed extra typical pyrolytic water derived from the secondary reaction of oxygen-containing functional groups (-OH, -COO-, -COOH- *etc*.). Finally, at a temperature above 800 °C, the emissions of main gases were ended earlier than that of CO and CO_2, indicating completeness with char formation.

The absorbance *versus* time profiles of the emitted gases, *e.g*., H_2O, CO_2, CO, CH_4 and C_2H_4, are shown in Figure 4. The H_2O emission profile during lignin pyrolysis showed different evolution peaks located at 117 °C (drying water) and 387 °C (pyrolysis water), which might be originating from condensation reactions.[5] The appearance of CO_2 occurring at a temperature of 385 °C was mainly due to the decarboxylation or decarbonylation reactions of lignin, which possess high content of carboxylic and carbonyl groups attached to aromatic and aliphatic structures.[6] The CO_2 profile patterns showed two prominent emission peaks at 503 °C and 708 °C, likely originating from thermal cracking of volatile aromatic compounds and/or freshly formed char.[10] The CO evolution pattern showed a first evolution peak at about 392 °C, as most of the solid oxygenated complexes are converted into gases at a temperature of about 400 °C. With rising temperature, the CO emission continuously increased and reached the maximum intensity at 754 °C due to *in situ* gasification of volatile aromatics. The release of CH_4 occurred in the temperature range of 350-650 °C, with a broad peak of emission centered at 392 °C, whereas the C_2H_4 evolution patterns occurred in a wide temperature range (300-900 °C) with a broad peak of emission centered at 389 °C.

In addition to the above-mentioned gases, the gaseous stream contained complex organic molecules, which could be formed and decomposed during lignin pyrolysis. For example, the asymmetric and symmetric stretching vibrations ν(C-H) at 2936 cm^{-1} were identified in the region between 3100 and 2800 cm^{-1}, and were assigned to methyl and methylene groups attached to the aryl rings and aliphatic chains. The ether band C-O at 1176 cm^{-1}, assigned to phenols, alcohols and ethers, was also identified in the original FTIR spectra. In addition, the absorption bands at about 1700 cm^{-1} were assigned to C=O stretching from aldehydes, ketones and acids during lignin pyrolysis. It was noted in Figure 5 that the maximum rates of evolution of both alkyl groups and oxygen-containing compounds occurred at about 400 °C as a consequence of EHL thermal degradation.

Kinetic analysis

The results obtained from thermogravimetric analysis were elaborated according to model-free methods to calculate the kinetic parameters (Table 1). The activation energy (Ea) and pre-exponential factor (A) were obtained by the FWO and KAS methods.

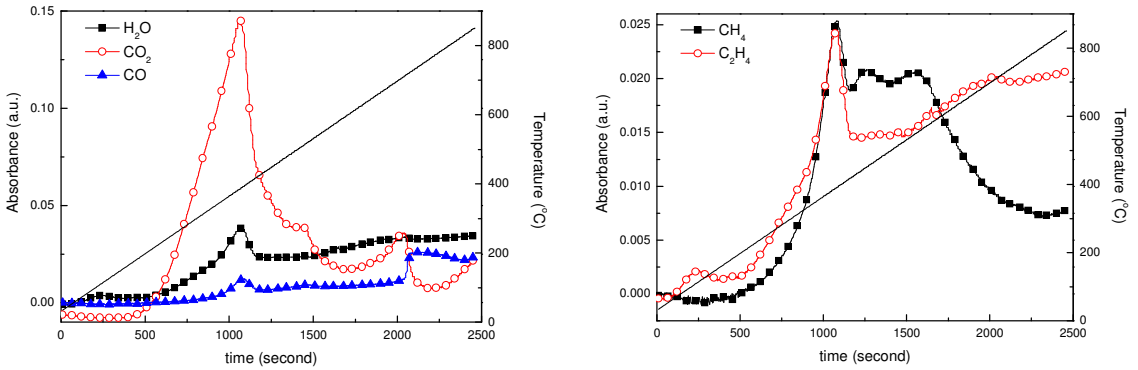

Figure 4: Absorbance *versus* time profiles of H_2O, CO_2, CO, CH_4 and C_2H_4 species evolved during EHL pyrolysis at 20 °C/min heating rate

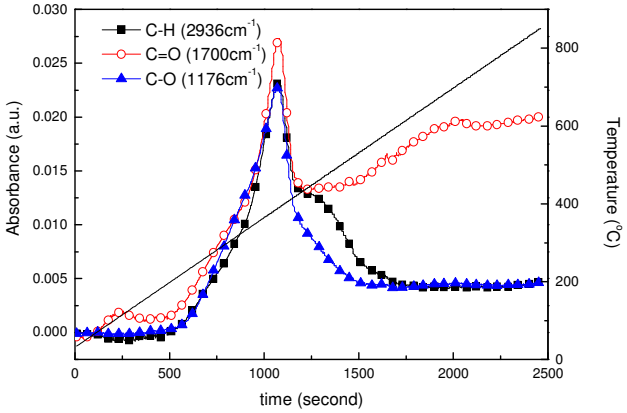

Figure 5: Absorbance *versus* time profiles of organic volatiles with C-H group, C=O group and C-O group evolved during EHL pyrolysis at 20 °C/min heating rate

FWO method

The kinetic parameters obtained by the FWO method were calculated according to Equation (8), for a given value of conversion, α. To determine the kinetic parameters, we chose the same value of α in the range from 0.1 to 0.6 for all the curves at different heating rates. The FWO plots of $\ln(\beta_i)$ *versus* $1000/T_{\alpha i}$ (K^{-1}) for different values of conversion are shown in Figure 6a. The apparent activation energies were obtained from the slope and the pre-exponential factors from the intercept of the regression line were given in Table 2. The calculated squares of the correlation coefficient, R^2, corresponding to the linear fittings in Figure 6a, were in the range from 0.96 to 0.99.

KAS method

The kinetic parameters for EHL pyrolysis were calculated using the KAS method according to Equation (9), for a given value of conversion, α. Similarly, we chose the same value of α in the range from 0.1 to 0.6 for all the curves at different heating rates and we found the corresponding temperature. The KAS plots of $\ln(\beta_i/T_{\alpha i}^2)$ *versus* $1000/T_{\alpha i}$ (K^{-1}) for different values of conversion are shown in Figure 6b. The apparent activation energies were obtained from the slope and the pre-exponential factors from the intercept of the regression line were given in Table 2. The calculated squares of the correlation coefficient, R^2, corresponding to the linear fittings in Figure 6b, were in the range from 0.96 to 0.99.

Table 1
Parameter values of EHL in FWO formula and KAS formula

Conversion, α	β (K/min)	Tα(K)	$1/T_\alpha \times 10^{-3}(K^{-1})$	Lnβ	$Ln(\beta/T_\alpha^2)$
0.1	10	521.73	1.92	2.30	-10.21
	20	529.72	1.89	3.00	-9.55
	30	541.34	1.85	3.40	-9.19
	40	544.53	1.84	3.69	-8.91
	50	549.68	1.82	3.91	-8.71
0.15	10	546.02	1.83	2.30	-10.30
	20	554.24	1.80	3.00	-9.64
	30	564.12	1.77	3.40	-9.27
	40	567.59	1.76	3.69	-8.99
	50	571.79	1.75	3.91	-8.79
0.2	10	565.12	1.77	2.30	-10.37
	20	573.52	1.74	3.00	-9.71
	30	582.28	1.72	3.40	-9.33
	40	586.01	1.71	3.69	-9.06
	50	589.23	1.70	3.91	-8.85
0.25	10	581.80	1.72	2.30	-10.43
	20	589.80	1.70	3.00	-9.76
	30	597.88	1.67	3.40	-9.39
	40	601.69	1.66	3.69	-9.11
	50	604.29	1.65	3.91	-8.90
0.3	10	595.02	1.68	2.30	-10.47
	20	603.74	1.66	3.00	-9.81
	30	611.20	1.64	3.40	-9.43
	40	615.10	1.63	3.69	-9.15
	50	617.38	1.62	3.91	-8.94
0.35	10	605.66	1.65	2.30	-10.51
	20	614.97	1.63	3.00	-9.85
	30	622.34	1.61	3.40	-9.47
	40	626.31	1.60	3.69	-9.19
	50	628.52	1.59	3.91	-8.97
0.4	10	614.40	1.63	2.30	-10.54
	20	624.04	1.60	3.00	-9.88
	30	631.64	1.58	3.40	-9.50
	40	635.65	1.57	3.69	-9.22
	50	638.01	1.57	3.91	-9.00
0.45	10	621.85	1.61	2.30	-10.56
	20	631.70	1.58	3.00	-9.90
	30	639.55	1.56	3.40	-9.52
	40	643.65	1.55	3.69	-9.25
	50	646.20	1.55	3.91	-9.03
0.5	10	628.82	1.59	2.30	-10.59
	20	638.63	1.57	3.00	-9.92
	30	646.67	1.55	3.40	-9.54
	40	650.85	1.54	3.69	-9.27
	50	653.59	1.53	3.91	-9.05
0.55	10	636.14	1.57	2.30	-10.61
	20	645.57	1.55	3.00	-9.94
	30	653.74	1.53	3.40	-9.56
	40	657.94	1.52	3.69	-9.29
	50	660.92	1.51	3.91	-9.08
0.6	10	647.34	1.54	2.30	-10.64
	20	653.88	1.53	3.00	-9.97
	30	662.21	1.51	3.40	-9.59
	40	665.81	1.50	3.69	-9.31
	50	668.95	1.49	3.91	-9.10

Table 2
Activation energy and Arrhenius constants obtained by FWO and KAS methods for EHL pyrolysis

Conversion, α	FWO method			KAS method		
	E/(kJ/mol)	LnA/min^{-1}	R^2	E/(kJ/mol)	LnA/min^{-1}	R^2
0.10	124.50	26.05	0.9683	122.08	25.36	0.9635
0.15	148.45	30.49	0.9808	146.88	29.64	0.9783
0.20	169.20	34.14	0.9877	168.40	33.18	0.9862
0.25	190.50	37.82	0.9882	190.54	36.79	0.9869
0.30	201.32	39.34	0.9927	201.71	38.16	0.9919
0.35	204.52	39.41	0.9937	204.89	38.05	0.9930
0.40	204.26	38.92	0.9939	204.47	37.36	0.9933
0.45	203.36	38.40	0.9943	203.40	36.64	0.9937
0.50	204.70	38.36	0.9944	204.69	36.44	0.9938
0.55	209.52	38.97	0.9940	209.63	36.94	0.9933
0.60	242.59	44.76	0.9770	244.26	42.86	0.9749
Average value	191.17	36.97		191.00	35.58	

*R^2 corresponding to linear fittings

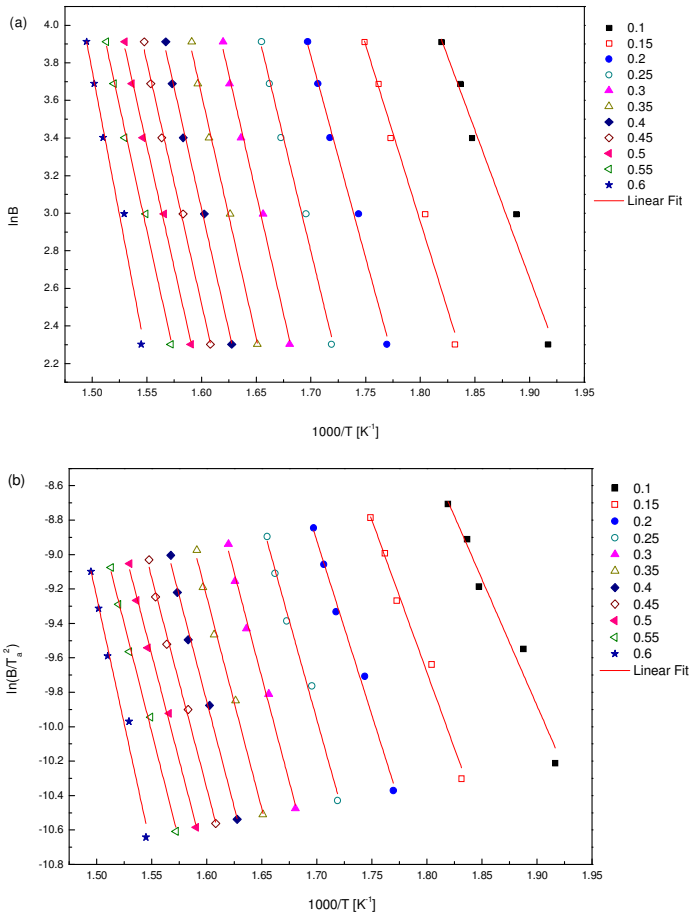

Figure 6: Linearization curves by FWO (a) method and KAS (b) method for EHL pyrolysis

In Table 2, we can observe that the apparent activation energies for the pyrolysis of EHL are not similar for all the conversions, which indicates the existence of a complex multistep mechanism that occurs in the substrate. The average value of the apparent activation energy is

191.0-191.2 kJ mol^{-1}, according to the FWO and KAS methods, respectively. It was shown that the values of the kinetic parameters obtained by both methods were analogous and could be successfully applied to understand the complex degradation mechanism of EHL.

CONCLUSION

In this paper, a comprehensive study of EHL pyrolysis kinetics is presented. Thermogravimetric analysis was investigated under helium atmosphere at different heating rates of 10-50 °C min^{-1}. Thermal decomposition of EHL proceeds in three stages: water evaporation, devolatilization of organic volatiles and char formation. It was found that the main pyrolysis process occurred at about 200-600 °C. The effect of the heating rate on the TG and DTG curves was also investigated. The activation energy and the pre-exponential factor were calculated by the FWO and KAS methods, and dependent on conversion due to the complex mechanism of reaction during EHL pyrolysis. The values of the activation energy obtained by the two methods were in good agreement, *e.g*., 191.2 kJ mol^{-1} and 191.0 kJ mol^{-1}, respectively. Experimental results showed that the model-free methods could describe the complexity of the EHL thermal decomposition process. However, more work is needed to effectively utilize the rich information obtained from this analysis and to quantitatively investigate the pyrolytic mechanism for practical applications.

ACKNOWLEDGEMENTS: Financial support from the National Natural Science Foundation of China (No. 21774059), Priority Academic Program Development (PAPD) of Jiangsu Higher Education Institutions, the opening funding of Jiangsu Key Lab of Biomass-based Green Fuels and Chemicals, and College Students' Practice and Innovation Training Project (201810298058Z).

REFERENCES

[1] X. Jiang, Q. Lu, B. Hu, J. Liu, C. Dong *et al*., *Fuel*, **215**, 386 (2018).
[2] Y. Furutani, S. Kudo, J. Hayashi and K. Norinaga, *Fuel*, **212**, 515 (2018).
[3] A. Galano, J. Aburto, J. Sadhukhan and E. Torres-García, *J. Anal. Appl. Pyrol*., **128**, 208 (2017).
[4] S. Wang, H. Lin, B. Ru, W. Sun, Y. Wang *et al*., *J. Anal. Appl. Pyrol*., **108**, 78 (2014).
[5] B. Li, W. Lv, Q. Zhang, T. Wang and L. Ma, *J. Anal. Appl. Pyrol*., **108**, 295 (2014).
[6] Q. Liu, S. Wang, Y. Zheng, Z. Luo and K. Cen, *J. Anal. Appl. Pyrol*., **82**, 170 (2008).
[7] Z. Luo, S. Wang and X. Guo, *J. Anal. Appl. Pyrol*., **95**, 112 (2012).
[8] D. Shen, J. Hu, R. Xiao, H. Zhang, S. Li *et al*., *Bioresour. Technol*., **130**, 449 (2013).
[9] L. Chen, X. Wang, H. Yang, Q. Lu, D. Li *et al.*, *J. Anal. Appl. Pyrol*., **113**, 499 (2015).
[10] J. Zhao, X. Wang, J. Hu, Q. Liu, D. Shen *et al*., *Polym. Degrad. Stabil*., **108**, 133 (2014).
[11] M. Brebu, T. Tamminen and I. Spiridon, *J. Anal. Appl. Pyrol*., **104**, 531 (2013).
[12] P. Simon, *J. Therm. Anal. Calorim*., **76**, 123 (2004).
[13] N. Sbirrazzuoli, L. Vincent, A. Mija and N. Guio, *Chem. Intell. Lab. Syst*., **96**, 219 (2009).
[14] S. Katarzyna, B. Pietro and F. Francesco, *Appl. Energ*., **97**, 491 (2012).
[15] S. Vyazovkin and C. A. Wight, *Thermochim. Acta*, **340**, 53 (1999)
[16] Z. Ma, J. Wang, Y. Yang, Y. Zhang, C. Zhao *et al*., *J. Anal. Appl. Pyrol*., **134**, 12 (2018).
[17] B. Joffres, D. Laurenti, N. Charon, A. Daudin and A. Quignard, *Oil Gas Sci. Technol*., **68**, 753 (2013).
[18] L. Yang, K. Seshan and Y. Li, *Catal. Today*, **298**, 276 (2017).
[19] F. Collard and J. Blin, *Renew. Sust. Energ. Rev*., **38**, 594 (2014).
[20] S. Kang, X. Li, J. Fan and J. Chang, *Renew. Sust. Energ. Rev*., **27**, 546 (2013).
[21] C. Lai, M. Tu, Z. Shi, K. Zheng, L. G. Olmos *et al*., *Bioresour. Technol*., **163**, 320 (2014).
[22] G. Guo, S. Li, L. Wang, S. Ren and G. Fang, *Bioresour. Technol*., **135**, 738 (2013).
[23] X. Gu, X. Zhou, M. Wu, X. Wang, Y. Chen *et al*., *Cellulose Chem. Technol*., **51**, 387 (2017).
[24] X. Gu, X. Ma, L. Li, C. Liu, K. Cheng *et al.*, *J. Anal. Appl. Pyrol*., **102**, 16 (2013).
[25] K. J. Laidler, "Chemical Kinetics", McGraw-Hill Book Company, 1965.
[26] J. Flynn and L. Wall, *J. Polym. Sci*., *B*: *Polym. Phys*., **4**, 323 (1966).
[27] T. Ozawa, *Bull. Chem. Soc. Jpn*., **38**, 1881 (1965).
[28] H. Kissinger, *J. Res. Nat. Bur. Stand*., **57**, 217 (1956).
[29] A. Galano, J. Aburto, J. Sadhukhan and E. Torres-García, *J. Anal. Appl. Pyrol*., **128**, 208 (2017).
[30] J. A. Caballero, R. Font and A. Marcilla, *J. Anal. Appl. Pyrol*., **36**, 159 (1996).
[31] S. S. Abdullah, S. Yusup, M. M. Ahmad, A. Ramli and L. Ismail, *Int. J. Chem. Biol. Eng*., **4**, 12 (2010).